1996MNRAS.281L..75E

Mon. Not. R. Astron. Soc. **281,** L75–L81 (1996)

Identification of a gravitationally lensed $z = 2.515$ star-forming galaxy

T. M. D. Ebbels,[1] J.-F. Le Borgne,[2] R. Pelló,[2] R. S. Ellis,[1] J.-P. Kneib,[1] I. Smail[3] and B. Sanahuja[4]

[1]*Institute of Astronomy, Madingley Road, Cambridge CB3 0HA*
[2]*Observatoire Midi-Pyrénées, 14 Av. E. Belin, 31400 Toulouse, France*
[3]*The Observatories of the Carnegie Institution of Washington, 813 Santa Barbara Street, Pasadena, CA 91101-1292, USA*
[4]*Departament D'Astronomia i Meteorologia, Universitat de Barcelona, Diagonal 648, 08028 Barcelona, Spain*

Accepted 1996 May 21. Received 1996 May 7; in original form 1996 February 5

ABSTRACT

We discuss the optical spectrum of a multiply imaged arc resolved by the *Hubble Space Telescope* in the $z = 0.175$ cluster A2218. The spectrum, obtained with LDSS-2 on the 4.2-m William Herschel Telescope, reveals the source to be a galaxy at a redshift $z = 2.515$, in excellent agreement with the value predicted by Kneib et al. on the basis of their inversion of a highly constrained mass model for the lensing cluster. The source is extremely blue in its optical–infrared colours, consistent with active star formation, and the spectrum reveals absorption lines characteristic of a young stellar population. Of particular significance is the absence of Lyα emission but the presence of a broad Lyα absorption. The spectrum is similar to that of other, much fainter, galaxies found at high redshift by various techniques, and illustrates the important role that lensing can play in detailed studies of the properties of distant galaxies.

Key words: galaxies: clusters: individual: A2218 – galaxies: evolution – cosmology: observations – gravitational lensing.

1 INTRODUCTION

Considerable progress has been made recently, from systematic redshift surveys of faint galaxies, in understanding the evolutionary properties of galaxies out to redshifts $z \simeq 1$ (Colless 1995; Lilly et al. 1996; Ellis et al. 1996). Beyond this strategic barrier, a variety of new techniques promise to extend our understanding to higher redshift. Cowie, Hu & Songaila (1995) have extended the direct spectroscopic approach for K-limited samples to $z \simeq 1.6$, and shown that a number have sufficiently strong star formation to account for a high fraction of the present-day stellar density. A drawback of this approach, as a way of finding representative distant galaxies, is that only a minority of a magnitude-limited sample, even at the faint limits now reachable with 10-m-class telescopes, lie beyond $z \simeq 1$. Presumably even fainter surveys would be required to uncover significant numbers of $z > 2$ galaxies. Although systematic, this method may not be the most efficient way to locate high-redshift galaxies.

In contrast, Steidel et al. (1996) have shown that very high-redshift sources can be effectively isolated from multi-band photometry using the Lyman limit as a discriminator. However, the Lyman limit ($\lambda_{\rm rest} = 912$ Å) only becomes amenable to optical detection at redshifts $z \gtrsim 2.8$ and thus, although it is undoubtedly a very powerful technique, any comparison of such a distant sample with one similarly selected at a lower redshift will remain an observational challenge for the UV capabilities of the *Hubble Space Telescope* (*HST*) (e.g. Conti, Leitherer & Vacca 1996). Finally, one must consider the searches for damped Lyα absorbers (e.g. Wolfe et al. 1995). The main disadvantage here is contamination of the spectrum by the QSO light which inevitably hampers detailed investigation of the absorbing galaxy. Secondly, one has to contend with an uneven selection function in redshift produced by the varying detectability of the absorption.

In this article we illustrate the important role that gravitational lensing can play in selecting distant galaxies over a large redshift range, spanning those covered by the methods discussed above. The principal advantage of lensing in this context is, of course, the boosting of the apparent magnitude of the faint galaxy. Early work in this direction was begun by Smail et al. (1993) who discussed the photometric properties of giant arcs of known redshift in the context of various evolutionary models. The unlensed magnitudes of

© 1996 RAS

© Royal Astronomical Society • Provided by the NASA Astrophysics Data System

1996MNRAS.281L..75E

the arcs in their sample are estimated to be fainter than those of the galaxies studied in the deepest current conventional 10-m samples (e.g. Cowie et al. 1995). Although it is well known that lensing conserves surface brightness, parts of the source smaller than the seeing disc do undergo a real surface brightness gain (see Ebbels et al., in preparation). Although this may not be as large as the formal lensing magnification, the spectroscopic gain in depth can be significant. Additionally, the spatial magnification enables distant sources to be resolved into their individual components using *HST* (Smail et al. 1996).

The data from *HST* have enabled the construction of very precise mass models for selected lensing clusters. A good example is the recent analysis of Abell 2218 ($z=0.175$) where the ground-based mass model of Kneib et al. (1995) was confirmed in exquisite detail from as many as seven multiply imaged sources resolved by *HST* in a 3-orbit exposure (Kneib et al. 1996, hereafter KESCS). The highly constrained mass model allowed KESCS to invert the lensing equations and predict redshifts for individual arclets readily recognized in the *HST* images. A number of the arclets were predicted to have redshifts $z>1$; as a way of isolating high-redshift sources, the technique will become more effective as higher redshift lenses are employed. As the inversion is a purely geometric technique, selection effects are less troublesome than with the alternative approaches. Some of the difficulties inherent in the optical detection of lensed galaxies are discussed in KESCS. Clearly it is important to verify the lensing inversion, where possible, and in this article we illustrate the potential of the method via the spectrum of a spectacular multiply imaged arc in Abell 2218 (#384 in the numbering scheme of Le Borgne, Pelló & Sanahuja 1992). The large magnification (almost 3 mag for this image) allows us to obtain the spectrum of a normal galaxy at high redshift. The redshift obtained, $z=2.515$, is in very good agreement with that predicted by the lensing model of KESCS.

A plan of the paper follows. In Section 2 we present the spectroscopic observations that lead to the redshift determination, and discuss its implications with respect to the inversion method discussed by KESCS. In Section 3 we discuss the broad-band photometric properties of the distant galaxy, and estimate the ongoing star formation rate and rest-frame luminosities. In Section 4 we return to the spectrum and interpret the various features in the context of the photometric data and UV spectra of nearby galaxies, and recent spectra of high-redshift sources. Section 5 summarizes the main conclusions of the paper.

2 SPECTROSCOPIC OBSERVATIONS AND REDSHIFT DETERMINATION

As part of a major effort to verify the lensing inversion method for Abell 2218 discussed by KESCS, we have secured for a large sample of faint arclets using the LDSS-2 multi-slit spectrograph at the William Herschel Telescope (WHT). A more complete description of these observations will be presented elsewhere (Ebbels et al., in preparation). The arclets were selected to be those with lensed magnitudes $B<25$ for which the inversion gave estimated redshifts $z_{\rm lensing}>0.4$. Although a colour selection was imposed to increase the chance of detecting [O II] emission in the spectral window of LDSS-2, this is immaterial in the present discussion.

The observations were conducted on the nights of 1995 May 28 and June 1. LDSS-2 was used in a conventional multi-slit mode with masks constructed with straight slits of width 1.5 arcsec configured in two orientations. The TEK-1 CCD was used (0.59 arcsec pixel^{-1}) and, in the case of this arc, a total exposure of 29.9 ks was obtained with the medium blue grism (5.3 Å pixel^{-1}, resolution $\simeq$12 Å), in conditions with seeing $\simeq$1–2 arcsec FWHM. This grism allows us to survey the range where Lyα was predicted to lie for arc #384 by Pelló et al. (1992) and Kneib et al. (1995) (3700–5300 Å; this range was not obtained in Pelló et al.'s FOS spectrum).

Standard data reduction was performed with the LEXT package (Colless et al. 1990; Allington-Smith et al. 1994). After debiasing, the data were median-combined, allowing for flexure effects of $\sim$1 pixel which affect the long exposures of a single field. Dispersed tungsten flat-fields were used to correct for variations in transmission along the slit, while wavelength calibration was achieved using a CuAr arc. In extracting the faint spectra, the light profile along the slit was used to fit the remaining background variations and isolate the object. Residual column-to-column deviations from this fit were removed linearly and the object rows summed with a Gaussian weighting to form an optically extracted spectrum. Finally, the spectra were approximately flux-calibrated using the standard LDSS-2 throughput curves.

The arc in question, #384 (Fig. 1a, opposite) in the photometric catalogue of Le Borgne et al. (1992), is one of the most spectacular in appearance in the *HST* image presented by KESCS. The mirror symmetry apparent in the WFPC-2 data verifies the earlier suggestion (Kneib et al. 1995) that the arc represents the merging of two images across a critical line, the location of which can now be precisely determined. The mass model discussed by KESCS, which is highly constrained by six further multiply imaged features, strengthens the prediction (Kneib et al. 1995) of a counter-image to #384 on the other side of the central cD galaxy (object #468, Fig. 1b).

The location and orientations of the two images allowed KESCS to predict the inverted redshift and magnification of the source to reasonably high precision. Indeed, the redshift of #384 represents a crucial constraint because of the proximity of the arc to the critical line. On the basis of the mass model developed, the source is predicted to lie within the range $z_{\rm lensing}=2.8\pm0.3$, the uncertainty arising from the detail of the mass model, once constraints of the other multiply imaged systems in the cluster are considered. This prediction agrees well with that made from broad-band photometry and 5300–9000 Å low-resolution spectroscopy, at $2.6\lesssim z\lesssim3.6$, by Pelló et al. (1992).

The new redshift, when included in the model, does little to change the predicted magnification of each image [2.9 ± 0.3 in the case of the combined #384 images and 1.5 ± 0.1 in the case of #468. The larger error for #384 results from its proximity to the critical line, and thus increased sensitivity to its exact position and the slope of the mass profile (see KESCS). In calculating the properties of the unlensed source, we use the more reliable magnification of #468]. This leads to an *unlensed R* magnitude for

© Royal Astronomical Society • Provided by the NASA Astrophysics Data System

1996MNRAS.281L..75E

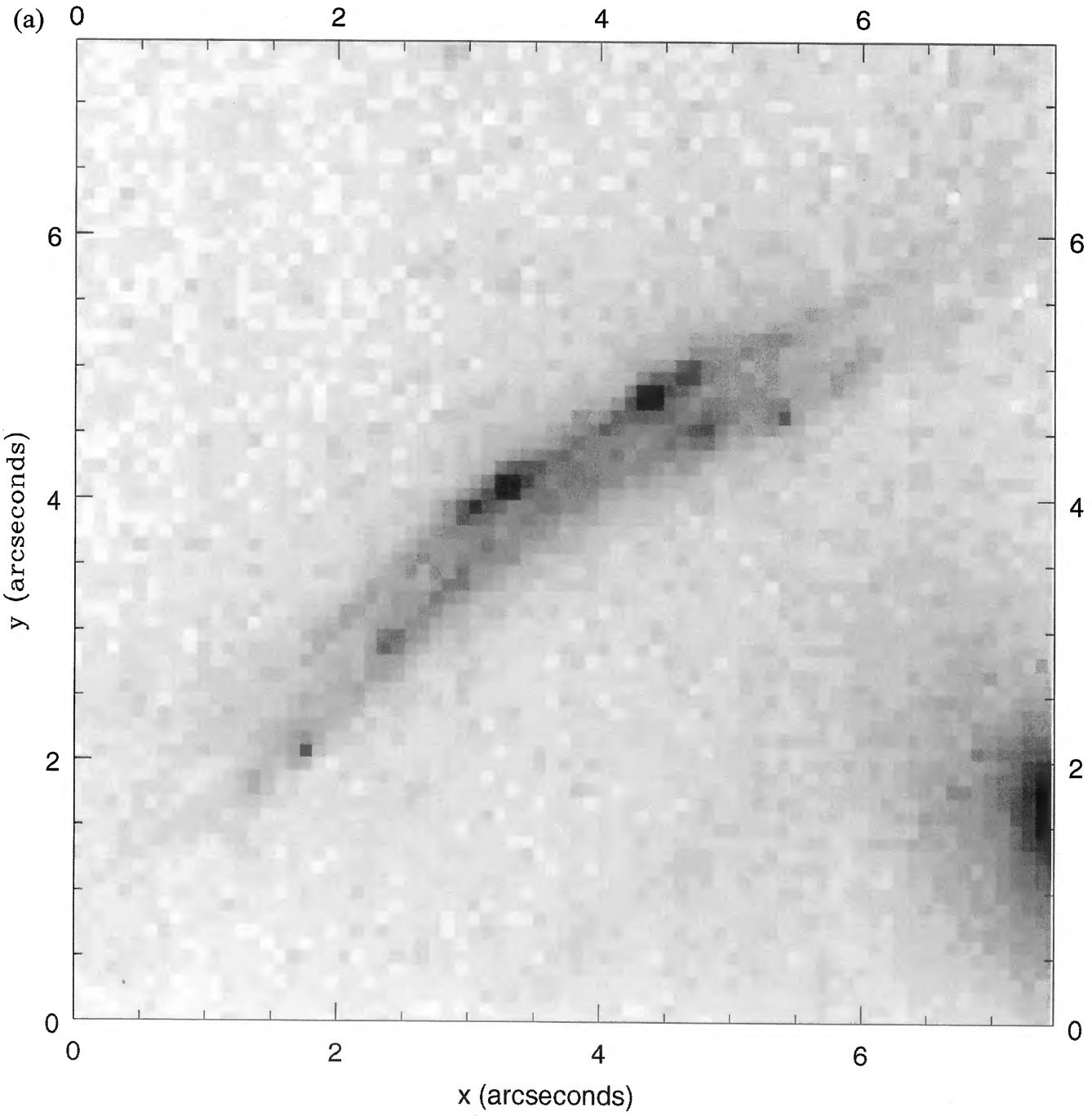


Figure 1. (a) WFPC-2 F702W image of arc #384 (after KESCS). (b) WFPC-2 F702W image of arc #468 considered by KESCS to be the counter-image of #384.

© Royal Astronomical Society • Provided by the NASA Astrophysics Data System

1996MNRAS.281L..75E

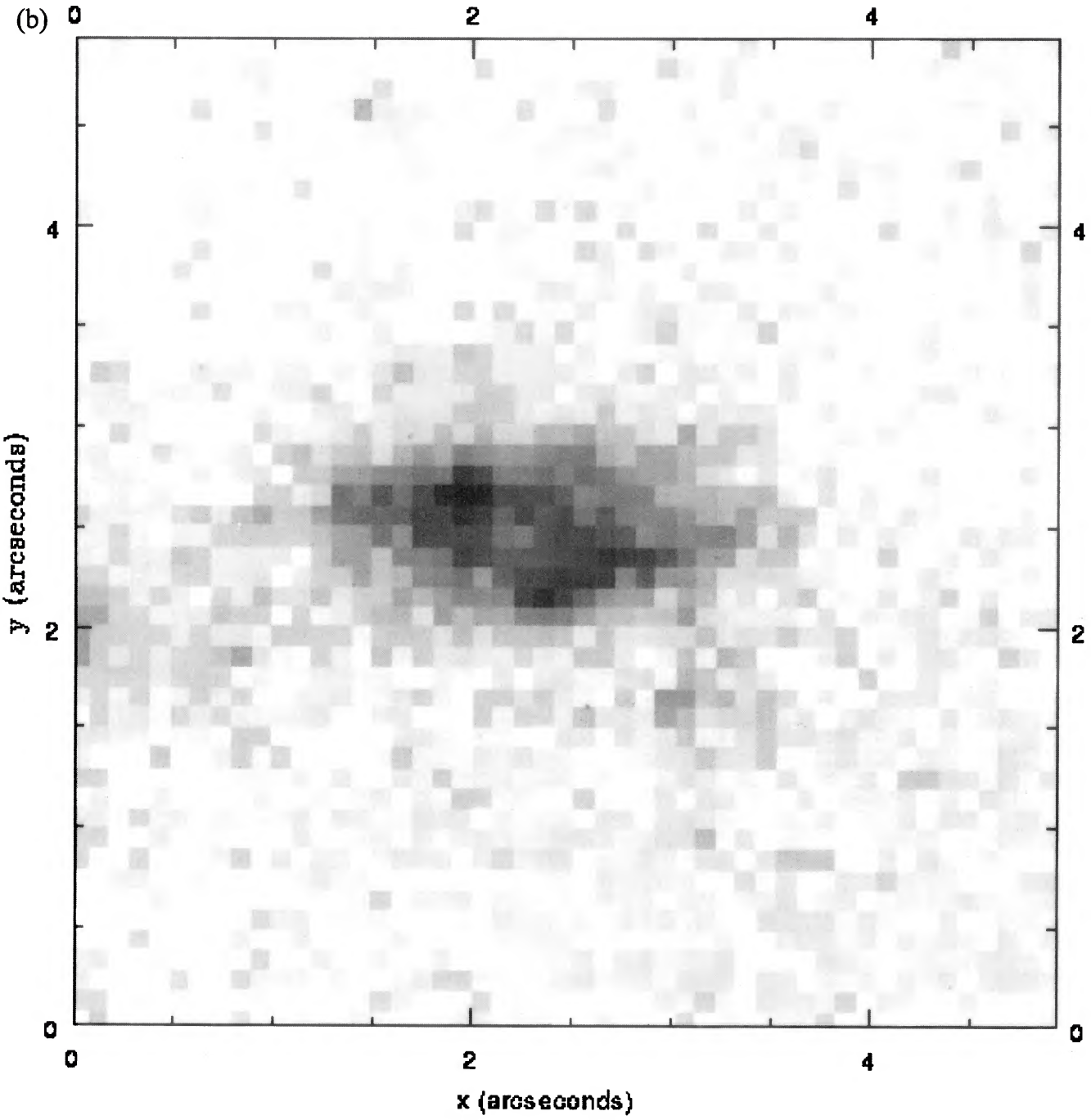


Figure 1 – *continued*

© Royal Astronomical Society • Provided by the NASA Astrophysics Data System

1996MNRAS.281L..75E

#384/#468 of 24.1 ± 0.2. As KESCS point out, #384 comprises two images of a source which itself appears to consist of two parallel components. #468 has the same distinctive parallel morphology, albeit less distorted by the gravitational shear. Since the source lies so close to a caustic in the source plane, any bright parts of it lying outside this caustic would be imaged only in #468. The absence of any such extra bright knots in #468 leads us to conclude that all high surface brightness parts of the source lie inside the caustic line.

The LDSS-2 spectrum for #384 is shown in Fig. 2 and has a very satisfactory signal-to-noise ratio. Although the integrated photometry indicates $R_{\rm tot}=21.2$, the mean surface brightness is only $\mu_R=23.4$ ($\simeq 7$ per cent of the La Palma night sky). Thus the observation represents a considerable challenge. The spectrum shows a number of strong ultraviolet features consistent with a redshift $z=2.515$, close to the predicted value. Most noticeable is the prominent feature at $\simeq 4250$ Å which arises from strong Lyα absorption. No emission lines are seen in the optical spectrum. With our new data, we find that the multiple-image hypothesis is reinforced by comparing the spectra of all three images. The two halves of #384 show no difference in spectral features, while the spectrum of #468 (Fig. 3), although noisy, is certainly compatible with that of #384. We return to a detailed discussion of the spectral features in the next section.

The verification of the inverted redshift, to within the estimated precision, illustrates the power of the lensing technique for isolating high-redshift galaxies as well as for determining the statistical redshift distribution of very faint sources. It also shows that the mass model for the cluster core is very well determined, and, in fact, further constrains it. The implications of the comparison of the lensing-predicted redshifts and spectroscopically determined ones will be presented in Ebbels et al. (in preparation), where the spectroscopic results from all the arclets secured in the WHT run will be collated and analysed.

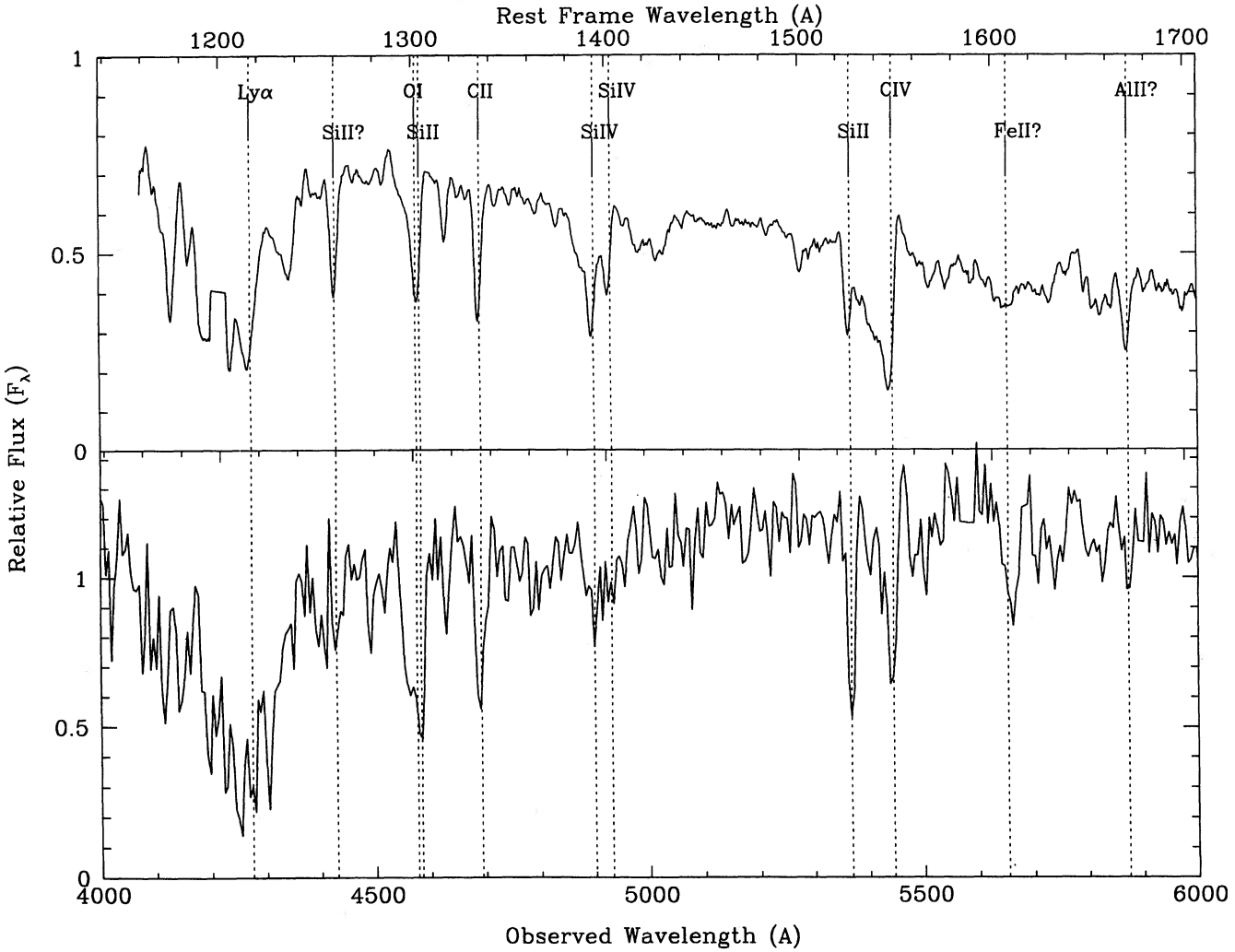


Figure 2. Bottom: LDSS-2 spectrum of the arc #384. Both strong and more tentative identifications of features indicating a redshift of $z=2.515\pm0.001$ are marked. Sky residuals near 5577 and 5892 Å have been truncated for clarity. Top: for comparison, the *HST* spectrum of a star-forming knot in NGC 1741 smoothed to the effective resolution of LDSS-2 (Conti et al. 1996). Many of the same features as in arc #384 are visible here, including metal lines and a broad Lyα line which does not reach the zero flux level. The truncated emission at $\simeq 1200$ Å is geocoronal Lyα.

© Royal Astronomical Society • Provided by the NASA Astrophysics Data System

1996MNRAS.281L..75E

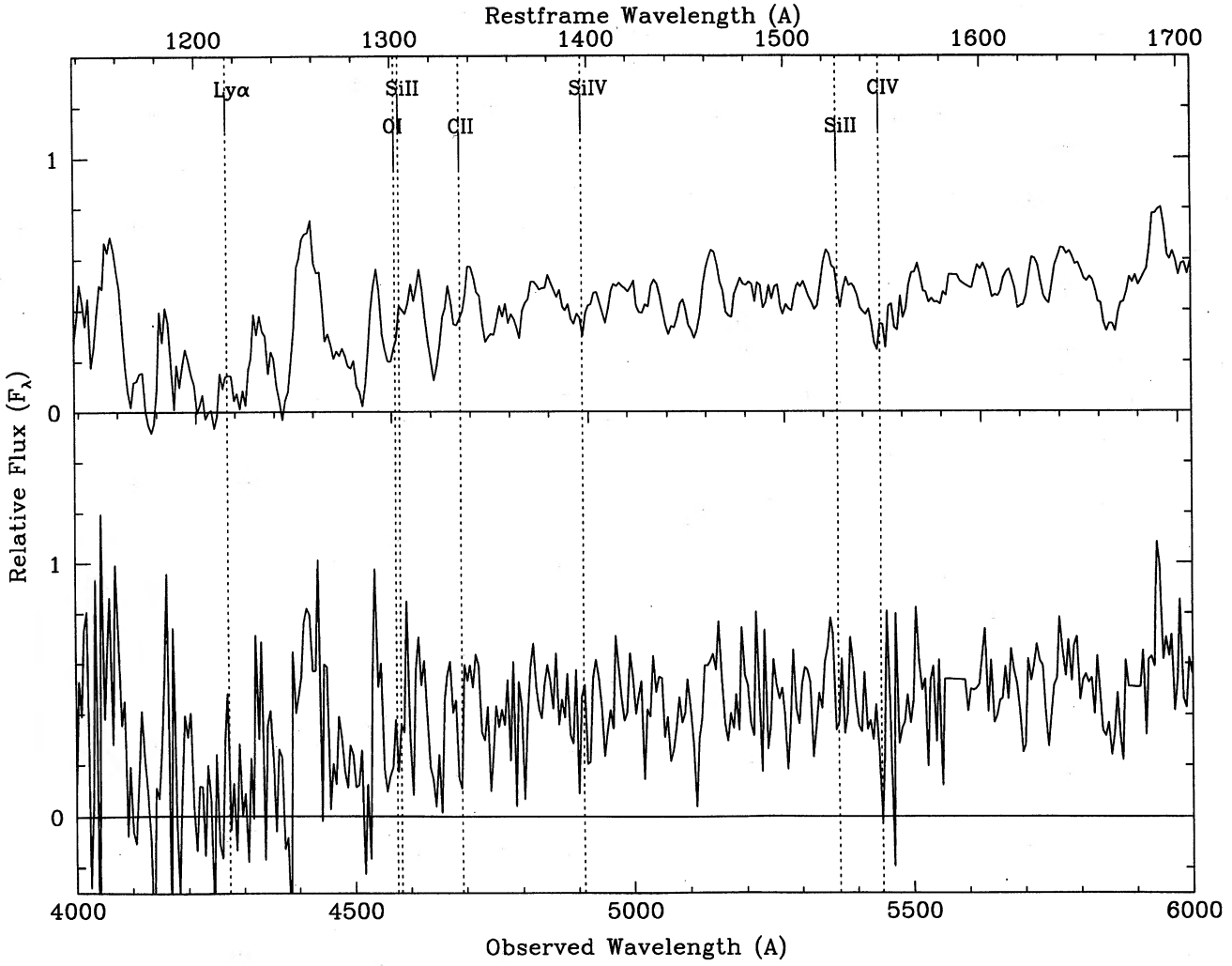


Figure 3. Bottom: LDSS-2 spectrum of the arc #468, showing that it is compatible with that of #384. Top: #468 spectrum smoothed with a boxcar of width 5 pixels. Positions of stronger lines appearing on the #384 spectrum are marked. Solid horizontal lines mark the zero levels.

3 PHOTOMETRIC PROPERTIES

Although there are now several examples of non-active galaxies with redshifts above 2, most can only be seen by virtue of their abnormal luminosities. The significant boosting of the source responsible for the arcs #384 + #468, together with the serendipitous way in which background galaxies are lensed, makes lensing a useful probe of normal galaxies at hitherto unexplored epochs, particularly if, as seems clear, further examples can be found in this way. We now illustrate, using this source as an example, what can be learnt from the photometric and spectroscopic properties of lensed high-redshift galaxies.

Multiband photometry from U to K' is presented for both #384 and #468 in Table 1, where the revised magnification is also given. The most reliable method to estimate the source luminosity is to use the infrared photometry to estimate the rest-frame optical luminosity. This is most suitably done with the J or K' photometry, which can yield the rest-frame U or R luminosity to reasonable precision. As $(J-K')_{\rm obs}$ maps closely on to $(U-R)_{\rm rest}$, it can be seen from Table 1 that the galaxy is intrinsically very blue, corresponding to a flat-spectrum source. To obtain the intrinsic $b_{\rm J_{rest}}$ luminosity of the source, a colour correction from $U_{\rm rest}$ or $R_{\rm rest}$ to $b_{\rm J_{rest}}$ is required, and this yields $M_{b_{\rm J}} = -22.2$ $(-23.0) \pm 0.5$, corresponding to a galaxy of $\simeq 8$–20 (16–40) $h_{50}^{-2} L^*_{b_{\rm J}}$ for $q_0 = 0.5$ (0.1) (Loveday et al. 1992). However, the blue magnitude is much influenced by star formation and, given its blue colours $[(U-R)_{\rm rest} \simeq (J-K')_{\rm obs} = 2.1]$, it is possible that the rest-frame K luminosity of our galaxy could be closer to L^* than suggested by the above $M_{b_{\rm J}}$ value.

The spectral energy distribution (SED) delineated by the broad-band photometry is plotted in Fig. 4, where we compare it with a synthetic spectrum produced by Bruzual & Charlot's (1993) code and with the smoothed SED of a nearby star-forming galaxy, NGC 4449 (Ellis 1984). These both show the SED to be consistent with that of an actively star-forming galaxy. Although the best model fit obtained was that of a burst (of age $\simeq 3 \times 10^8$ yr, no reddening), other models (including those with constant star formation) can also reproduce the gross features of the photometry, particularly given the freedom to invoke reddening, which has

© Royal Astronomical Society • Provided by the NASA Astrophysics Data System

1996MNRAS.281L..75E

Table 1. Optical and infrared photometry of #384 and #468. Values for μ_R and R are taken from KESCS, those for J and K' from Kneib et al. (1995), and those for *grz* from Le Borgne et al. (1992), where the likely errors are ± 0.1, ± 0.4 and ± 0.3 respectively. Values for *UVBi* are taken from new photometry obtained at the 5-m Palomar telescope (TEK CCD; seeing 1–1.5 arcsec; exposures of 2.5, 16.5, 5.8 and 21.7 ks respectively). Estimated errors are ± 0.1 in *BVi* and $\pm 0.3/\pm 0.6$ in U for #384/#468 respectively. Also listed is the relative magnification, $\delta_m = (m_{384} - m_{468})$, of the two images. The unlensed magnitude of the source may be obtained by adding the magnification M to the values in the table, where $M_{384} = 2.9 \pm 0.3$ and $M_{468} = 1.5 \pm 0.1$.

#	μ_R	U	B	g	V	R	r	i	z	J	K'
384	23.4	22.2	22.2	22.1	21.4	21.2	21.6	20.6	21.5	20.0	17.9
468	23.5	23.8	23.8	23.6	23.1	22.6	23.1	22.3	22.9	20.9	19.1
δ_m		1.6	1.6	1.5	1.7	1.4	1.5	1.7	1.4	0.9	1.2

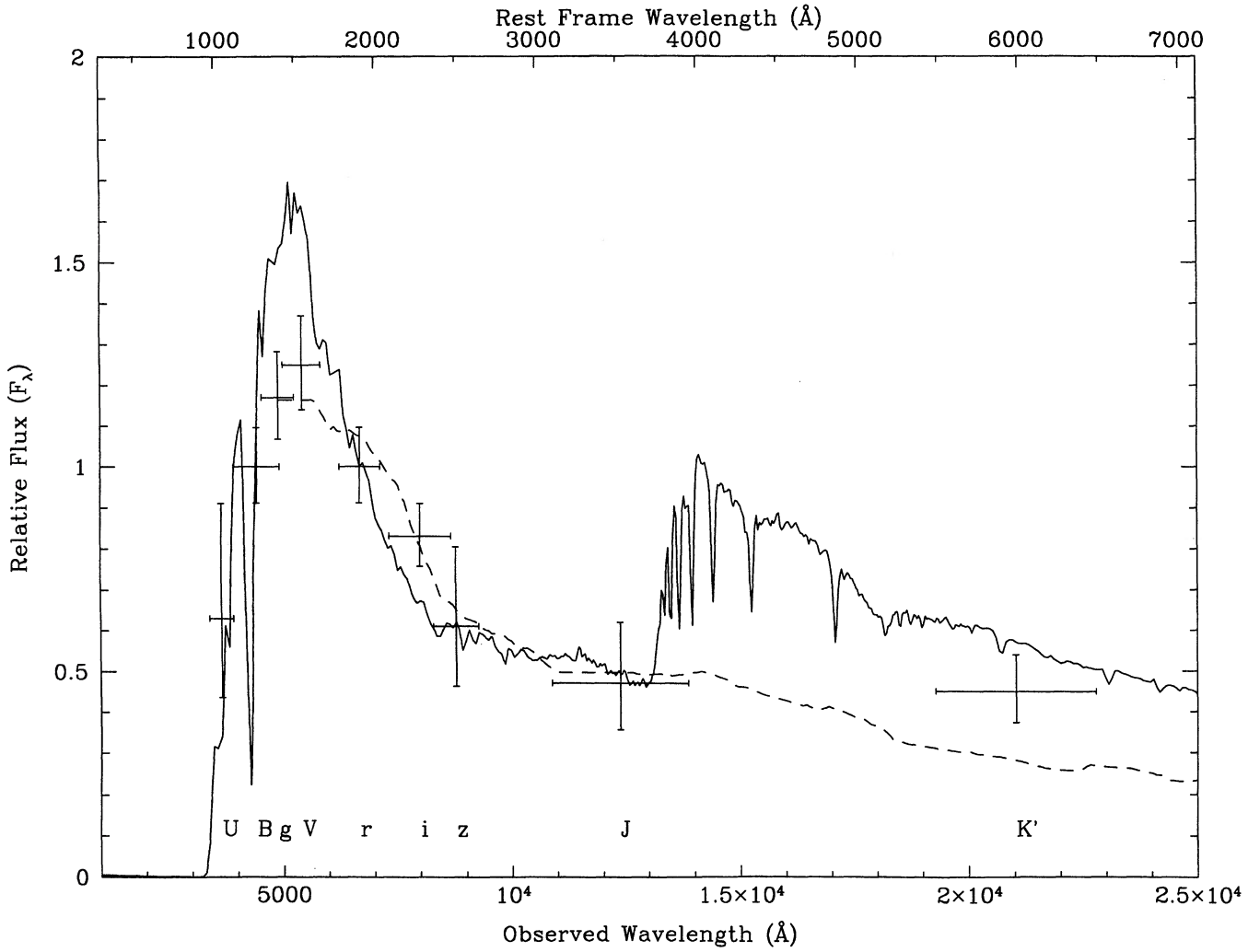


Figure 4. The spectral energy distribution of the $z = 2.515$ galaxy as determined from available broad-band photometry. The solid line represents the spectral energy distribution of a model of the burst type with no reddening and age of 0.286 Gyr. The dashed line shows the smoothed spectral energy distribution of NGC 4449, a well-studied local example of an actively star-forming galaxy.

sizeable effects at UV wavelengths (the exact nature of which is little known at these redshifts). At this redshift, the Lyman limit only just reaches the edge of the U band. Thus the drop in the photometry, although influenced by the Lyman break, cannot easily be compared with the $(U_n - G)$ cut from Steidel et al. (1996). Following Steidel et al., the UV flux can be used to derive an approximate ongoing star formation rate. In the case of a Salpeter initial mass function, (slope $\alpha = 2.35$, with $1 \leq M \leq 80\,M_\odot$), this amounts to $\simeq 7$–11 (15–24) $h_{50}^{-2}\ M_\odot\ yr^{-1}$ for $q_0 = 0.5$ (0.1), which is similar to the range seen in the Steidel sample and comparable to that in NGC 4449 when allowance for luminosity differences is made ($\simeq 8\ M_\odot\ yr^{-1}$: Thronson 1987).

As only the *HST* has the spatial resolution to detect adequately internal structures, and the WFPC-2 data are available only in a single band (F702W), no colour variations

© Royal Astronomical Society • Provided by the NASA Astrophysics Data System

1996MNRAS.281L..75E

along arc #384 can be seen. However, the presence of 'knots' in Fig. 2 is suggestive of luminous H II regions consistent with a galaxy undergoing strong star formation.

4 SPECTROSCOPIC PROPERTIES

The conclusions based on multiband photometry are also supported by analysis of the spectrum of #384 (Fig. 2). The most striking features are the broad Lyα absorption and the presence of several ultraviolet metal absorption lines. The latter features are typical of UV lines seen with *IUE* in the spectra of hot stars and nearby star-forming galaxies such as those catalogued by Kinney et al. (1993). As an illustration, Fig. 2 also shows the *HST* spectrum of a starburst knot in NGC 1741, a Wolf–Rayet galaxy at a distance of 77 h_{50}^{-1} Mpc (Conti et al. 1996). The spectral lines seen are similar to those in our source, while the luminosity of this knot at 1500 Å is a factor $\simeq 10$ fainter (as in the Steidel et al. 1996 sample).

Higher resolution data are required for a detailed analysis of the spectrum (e.g. definitive separation of stellar/interstellar absorption), but our data are sufficient to reveal several interesting aspects of this faint object. Using the redshift determined from the metal lines, it can be seen that the Lyα line is somewhat asymmetric (by $\simeq 200$ Å) on its blueward side. This may possibly be explained by a blend with metal lines such as Si III 1207 Å. There is also some evidence of further absorption at shorter wavelengths which could be Lyα absorption from foreground material. The Lyα absorption does not seem to reach a zero flux level, although the signal-to-noise ratio in the blue remains poor. Similar cases are seen in Kinney et al.'s sample, in the *HST* spectra of nearby galaxies discussed by Leitherer et al. (1996) and Conti et al. (1996), and in the high-redshift spectra of Steidel et al. (1996) and Yee et al. (1996). The claimed luminosity of the latter example is a factor of $\simeq 130$ (at 1500 Å) brighter than our source, strongly suggesting gravitational amplification by the cluster through which it is observed. This large factor allows the aquisition of a spectrum of much higher signal-to-noise ratio than the one presented here.

The strong stellar and interstellar lines seen by the above authors also appear strong in our spectrum, with a few exceptions, the most notable of these being the weakness of Si II 1260 Å compared with Si II 1527 Å. Although data of higher signal-to-noise ratio are required, this Si II ratio is the reverse of that seen in stellar spectra and raises the question of whether the 1527-Å line is contaminated, e.g. by a second component possibly associated with the double nature of the source mentioned in Section 2. From analyses of *IUE* stellar spectra and interstellar absorption of Magellanic Cloud stars (e.g. Savage & de Boer 1981), we conclude that most of the low-ionization lines (e.g. Si II, O I, Fe II, C II) are due to interstellar absorption, while those of higher ionization (e.g. C IV, Si IV) are mainly stellar, from late O to early B stars. In stars later than about B2, the doublet of 1526.7, 1533.4 Å becomes important and would have been resolved in our spectrum (cf. Rountree & Donneborn 1991), while, in the interstellar medium, only the line at 1526.7 Å is seen (as we observe). The absence of Lyα emission in a source with demonstrably active star formation confirms earlier suspicions that such emission can be attenuated by a number of processes (Charlot & Fall 1991, 1993). It is important to distinguish the configuration of our system from that of the QSO absorption scenario. In the QSO case, Lyα photons are scattered out of the beam by the absorber. In our case, the sources are embedded within the scattering medium and (as highlighted by Charlot & Fall) the extent of the attenuation depends on the relative abundances and geometry of the mixture of stars, gas and dust.

5 CONCLUSIONS

We have secured the redshift, $z=2.515$, of a multiply imaged arc in the rich cluster Abell 2218 which we believe to be the first confirmation of a redshift predicted by a cluster lensing model. The result strongly supports the precision of the lensing inversion technique developed by KESCS and further illustrates how gravitational lensing through well-constrained clusters can locate samples of high-redshift galaxies. The efficiency of this selection technique may be relatively low, given the surface density of high-redshift galaxies found by Steidel et al. and the cluster cross-section, coupled with the need for high-resolution imaging. However, this method is less susceptible to luminosity biases and redshift selection effects than are other techniques.

The source responsible for the lensed images appears to be a blue 8–20 L_{bj}^{*} galaxy, with an on-going star formation rate of 7–11 $M_{\odot}\,yr^{-1}$ which is consistent with that of similar sources found at higher redshift by Steidel and collaborators using the Lyman limit cut-off as a high-z locator. The spectrum reveals UV absorption lines which are consistent with the photometric properties. In particular, the Lyα line is particularly broad, suggesting that neutral gas is abundant within the galaxy. In conclusion, we believe that the spectral and photometric properties of this source are consistent with those expected of the objects responsible for high-redshift absorption along lines of sight to distant quasars.

ACKNOWLEDGMENTS

This paper is based on observations obtained with the William Herschel Telescope at the Observatorio del Roque de los Muchachos, La Palma. We thank Claus Leitherer, Howard Yee and Chuck Steidel for sharing their results with us prior to their publication. We acknowledge valuable discussions on the interpretation of ultraviolet spectra and photometry with Bob Carswell, Max Pettini and Alfonso Aragón-Salamanca. We especially note the help that Karl Glazebrook provided as a regular user of LDSS-2, which operates successfully thanks to the dedicated efforts of La Palma support staff and, in particular, Mike Breare. We are grateful to G. Bruzual for allowing the use of his code for the spectral evolution of galaxies. We also acknowledge financial support from the Particle Physics and Astronomy Research Council (TMDE and IS), the European Commission (JPK) and the DGICYT (Ministerio de Eduacion y Ciencia, Spain) (BS).

REFERENCES

Allington-Smith J. et al., 1994, PASP, 106, 983
Bruzual A., Charlot S., 1993, ApJ, 405, 538
Charlot S., Fall M., 1991, ApJ, 378, 471

© Royal Astronomical Society • Provided by the NASA Astrophysics Data System

1996MNRAS.281L..75E

Charlot S., Fall M., 1993, ApJ, 415, 580
Colless M., 1995, in Aragón-Salamanca A., Maddox S. J., eds, Wide Field Spectroscopy. World Scientific, Singapore, p.263
Colless M., Ellis R. S., Taylor K., Hook R. N., 1990, MNRAS, 253, 686
Conti P. S., Leitherer C., Vacca W. D., 1996, preprint
Cowie L. L., Hu E. M., Songaila A., 1995, Nat, 377, 603
Ellis R. S., 1984, in Gondhalekar P., ed., Spectral Evolution of Galaxies. RAL Publications, p.122
Ellis R. S., Colless M., Heyl J. S., Broadhurst T. J., Glazebrook K., 1996, MNRAS, in press
Kinney A. L., Bohlin R. C., Calzetti D., Panagia N., Wyse R. F. G., 1993, ApJS, 86, 5
Kneib J.-P., Mellier Y., Pelló R., Miralda-Escudé J., Le Borgne J.-F., Böhringer H., Picat J.-P., 1995, A&A, 303, 27
Kneib J.-P., Ellis R. S., Smail I. R., Couch W. J., Sharples R., 1996, ApJ, in press (KESCS)
Le Borgne J.-F., Pelló R., Sanahuja B., 1992, A&AS, 95, 87
Leitherer C., Vacca W. D., Conti P. S., Filippenko A. V., Robert C., Sargent W. L. W., 1996, ApJ, submittted
Lilly S. J., Le Fèvre O., Hammer F., Crampton D., 1996, ApJ, in press
Loveday J., Peterson B. A., Efstathiou G., Maddox S. J., 1992, ApJ, 390, 338
Pelló R., Le Borgne J.-F., Sanahuja B., Methez G., Fort B., 1992, A&A, 266, 6
Rountree J., Donneborn G., 1991, ApJ, 369, 515
Savage B. D., de Boer K. S., 1981, ApJ, 243, 460
Smail I., Ellis R. S., Aragón-Salamanca A., Soucail G., Mellier Y., Giraud E., 1993, MNRAS, 263, 628
Smail I., Dressler A., Kneib J.-P., Ellis R. S., Couch W. J., Sharples R. M., Oemler A., 1996, ApJ, in press
Steidel C. C., Giavalisco M., Pettini M., Dickinson M., Adelberger K. L., 1996, preprint
Thronson H. A., Hunter D. A., Telesco C. M., Harper D. A., Decher R., 1987, ApJ, 317, 180
Wolfe A. M., Lanzetta K. M., Foltz C. B., Chaffee F. H., 1995, ApJ, 454, 698
Yee H. K. C., Ellingson E., Bechtold J., Carlberg R. G., 1996, preprint

© 1996 RAS, MNRAS **281**, L75–L81

© Royal Astronomical Society • Provided by the NASA Astrophysics Data System